Conditional Correlations and Principal Regression Analysis for Futures

Armine Karamni
LadHyX, Ecole Polytechnique
Raphaël Benichou
Capital Fund Management
Michael Benzaquen
LadHyX, Ecole Polytechnique;
E-mail: michael.benzaquen@polytechnique.edu
Jean-Philippe Bouchaud
Capital Fund Management

Abstract
We explore the effect of past market movements on the instantaneous correlations between assets within the futures market. Quantifying this effect is of interest to estimate and manage the risk associated with portfolios of futures in a non-stationary context. We apply and extend a previously reported method called the principal regression analysis (PRA) to a universe of 84 futures contracts between 2009 and 2019. We show that the past up (resp. down) 10-day trends of a novel predictor – the eigen factor – tend to reduce (resp. increase) instantaneous correlations. We then carry out a multifactor PRA on sectorial predictors corresponding to the four futures sectors (indexes, commodities, bonds, and currencies), and show that the effect of past market movements on the future variations of the instantaneous correlations can be decomposed into two significant components. The first component is due to the market movements within the index sector, while the second component is due to the market movements within the bonds sector.

Keywords
conditional correlations, futures, principal regression analysis, risk, nonstationarity

1 Introduction

A crucial input for managing portfolio risk is the covariance matrix of the underlying assets. The empirical determination of this matrix is fraught with difficulties. One is that of sample size: when the length of the available time series is not very large compared to the number of assets in the portfolio, the empirical covariance matrix suffers from very significant biases. For example, the smallest eigenvalue is underestimated and the largest eigenvalue overestimated. The corresponding eigenvectors are also strongly affected by measurement noise. As a consequence, the realized risk of optimal (Markowitz-like) portfolios can be considerably larger than anticipated, see e.g. Bun et al. (2017).

But there is another, perhaps more fundamental reason for the out-of-sample risk being larger than expected: we do not live in a stationary world, described by a time-invariant covariance matrix. The covariance between assets evolves not only because the volatility of each asset changes over time (Cont, 2001) and reacts to the recent market trend (Bekaert and Wu, 2000; Bouchaud et al., 2001; Li et al., 2005), but also because the correlations themselves increase or decrease, depending on market conditions–see e.g. Ang and Chen (2002), Balogh et al. (2010), and Borland (2012). Sometimes these correlations jump quite suddenly, due to an unpredictable geopolitical event. The arch example of such a scenario is the Asian crisis in the fall of 1997, when the correlation between bonds and stock indexes abruptly changed sign and became negative–a "flight to quality" mode that has prevailed ever since (Wyart and Bouchard, 2007; Baur and Lucey, 2009). Whereas these events are hard to predict, some measurable indicators (or factors) do anticipate future changes of the correlation matrix. For example, as documented in Reigneron et al. (2011), the structure of the stock correlation matrix depends (statistically) on the past returns of the stock index (i.e. the average of all stock returns). The main effect is that the top eigenvalue of the correlation matrix increases after the whole market goes down (and vice versa). Correspondingly, the top eigenvector rotates towards $\mathbf{u}_0 = (1, 1, \dots, 1)/\sqrt{N}$ after a drop of the index.

The main idea of Reigneron et al. (2011) is to regress the instantaneous correlation matrix on the past value of one or several indicators I_a, as follows:

$$r_i(t)r_j(t) = \mathbf{C}_{ij} + \sum_a \mathbf{D}^a_{ij}(\tau) I_a(t-\tau) + \boldsymbol{\varepsilon}_{ij}(t,\tau)\,,$$

where $r_i(t)$ is the standardized return of asset i between t and $t+1$, $\boldsymbol{\varepsilon}$ a zero-mean noise term, and $I_a(t-\tau)$ the value of the indicator "a" fully known at time t. This indicator is assumed to be of zero mean, such that $\mathbf{C}$ is by definition the unconditional correlation matrix. Finally, $\mathbf{D}^a(\tau)$ is a matrix that measures the sensitivity of the instantaneous correlation matrix to indicator I_a lagged by τ. Low rank approximations of the $\mathbf{D}^a(\tau)$ matrices allow one to build intuitive and parsimonious models of how correlations are affected by the past. The eigenvalues and eigenvectors of this matrix are expected to describe the impact of $I_a(t-\tau)$ on correlations in a more precise way than what one would obtain by separate examination of the slope coefficients $\mathbf{D}_{i,j}(\tau)$. This protocol has been dubbed principal regression analysis (PRA) in Reigneron et al. (2011), and has the virtue of being much easier to calibrate and interpret than dynamical conditional correlation (DCC) models, see e.g. Engle (2002).

The aim of the present study is to extend to futures markets the analysis of Reigneron et al. (2011), which was devoted to individual stocks. This is interesting for different reasons. First, the CTA (commodity trading advisor) industry routinely deals with portfolios of futures, and the risk of these portfolios is obviously an important aspect CTA funds want to monitor and control. Second, most stocks are positively correlated and, correspondingly, the top eigenvector of the correlation matrix always remains close to the uniform mode $\mathbf{u}_0$. This is not the case in the universe of futures contracts. For example, as mentioned above, stock indexes and bonds are typically negatively correlated (at least since 1998).

In this paper, we apply a PRA to the universe of futures contracts, and elicit the main factors affecting the structure of the corresponding correlation matrix. Whereas the dynamical structure of the correlation matrix of stock returns has been discussed in several studies, using different methods, we are not aware of similar investigations of futures returns. We first analyze the simplest case of a single factor, that we choose to be a "hand-made" index I_0, where stock indexes, currencies (vs. dollar), and commodities all have the same positive weight, and bonds have a negative weight of equal magnitude. We study the timescale over which the return of this index should be measured such that the effect on the correlation matrix is strongest, and find ≈ 10 days. We then replicate the analysis with an index constructed from the top eigenvector of $\mathbf{C}$ which is close to, but not identical to I_0, and find that the quality of the prediction is increased. Finally, we run a multivariate PRA using four factors, namely the past returns of the four relevant sectors in the universe of futures: stock indexes, bonds, currencies, and commodities. This allows us to get a more complete picture of the mechanisms leading to a change in the correlation structure of futures markets.

2 Data and notation

The data that we use are daily returns of $N = 84$ different futures, from $t_{beg} = 1/1/2009$ to $t_{end} = 1/1/2019$. The list of the different futures is given in Appendix A. None of the chosen assets are exchanged on the Asian futures market, in order to avoid spurious correlations between returns labeled with different dates, arising from the offsets in the market opening times.

The futures that we consider are classified in four different sectors: indexes (IDX), commodities (CMD), bonds (YLD), and foreign exchange rates (FXR). In the FXR sector, all currencies are defined with respect to the US dollar.

The daily returns at time t are defined as the difference between the prices at time t and $t-1$, divided by the standard deviation of the price estimated using the last 30 days.[1] They are denoted by $r_k(t)$, where k indexes a given contract. We also redefine these returns so as to have zero mean and unit standard deviation:

$$r_k(t) \leftarrow \frac{r_k(t) - \langle r_k \rangle}{\sigma_k} \tag{1}$$

where $\langle r_k \rangle$ denotes the average return over the time window T and σ_k its standard deviation.

We also define the vector of returns $\mathbf{r}(t) \coloneqq (r_1(t), \ldots, r_N(t))^\intercal \in \mathbb{R}^N$, and the instantaneous correlation matrix

$$\rho_{i,j}(t) \coloneqq r_i(t) r_j(t). \tag{2}$$

We denote by $\mathbf{R}$ the matrix with $\mathbf{r}(t)$ as its tth column. The futures market index at day t is denoted by $I_0(t)$ and is defined as

$$I_0(t) \coloneqq \frac{1}{N} \sum_{i=k}^{N} s_k r_k(t) \tag{3}$$

where

$$s_k = \begin{cases} 1 & \text{if } k \in \text{YLD} \\ -1 & \text{if } k \notin \text{YLD} \end{cases} \tag{4}$$

and YLD denotes the set of futures in the bonds sector. This sign flip anticipates the fact that the top eigenvector of the correlation matrix has a positive sign on IDX, CMD, and FXR sectors and a negative sign on YLD.

For F $\in$ {IDX, YLD, CMD, FXR}, we define the sub-index $I_F(t)$ as

$$I_F(t) \coloneqq \frac{1}{|F|} \sum_{k \in F} r_k(t). \tag{5}$$

All factors (3) and (5) have zero mean, as the returns are centered. We further scaled them to be of unit variance.

The eigenvalues of an $N \times N$ symmetric matrix $\mathbf{A}$ are ranked in descending order and denoted by

$$\lambda^{\mathbf{A}}_1 \geq \cdots \geq \lambda^{\mathbf{A}}_N. \tag{6}$$

The corresponding unit-norm eigenvectors are denoted by $\mathbf{v}^{\mathbf{A}}_1, \ldots, \mathbf{v}^{\mathbf{A}}_N$.

Before turning to our PRA, we analyze the average correlation matrix $\mathbf{C} = (T-1)^{-1}\mathbf{R}^\intercal\mathbf{R}$ obtained from the data. It is depicted in Figure 1(a), sorted by sectors and subsectors. In the same figure we also show a version of this matrix with averaged correlations within individual subsectors (Figure 1b) and sectors (Figure 1c). The spectrum of $\mathbf{C}$ is shown in Figure 2(a). The eigenvectors associated with the largest eigenvalue (market mode) and second largest eigenvalue are visually represented in Figures 2(b) and (c), respectively. We find $\lambda^{\mathbf{C}}_1 = 19.08$ and $\lambda^{\mathbf{C}}_2 = 8.59$.

Let us introduce $\mathbf{e}_0$, the uniform mode for our pool of futures. Given that assets in the YLD sector are anti-correlated with the rest of the pool's assets (see Figure 2b), we define it as

$$\mathbf{e}_0 = N^{-1/2}(s_k)_{1 \leq k \leq N} \tag{7}$$

where s_k is defined in (4). The top eigenvector is such that $\mathbf{e}_0 \cdot \mathbf{v}^{\mathbf{C}}_1 = 0.90$, meaning that the eigenvector $\mathbf{v}^{\mathbf{C}}_1$ is indeed quite similar to the uniform mode.

Figure 1: (a) Empirical correlation matrix C for the futures data used in the present paper. (b) Subsector-averaged version. (c) Sector-averaged version.

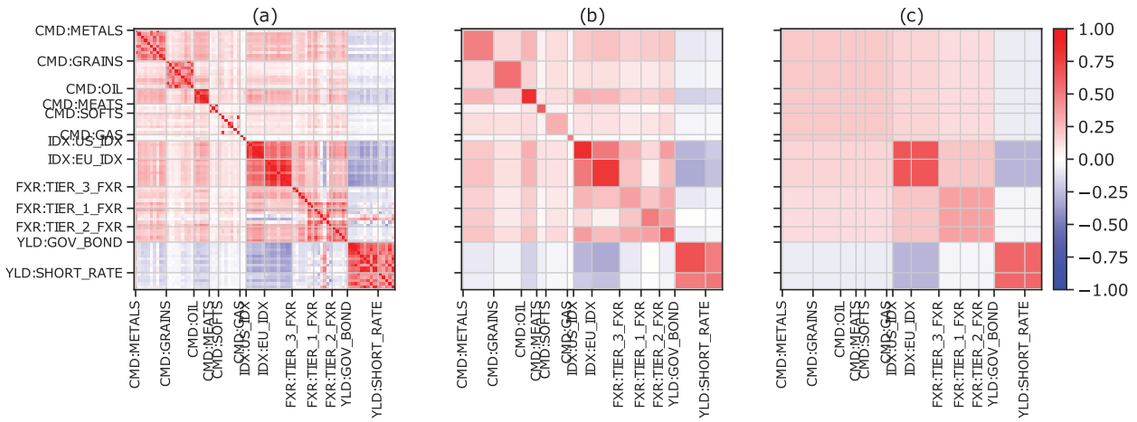

Figure 2: (a) Normalized spectrum of the empirical correlation matrix. (b, c) Visual representation of the two dominant eigenvectors of the empirical correlation matrix titled with their associated eigenvalues.

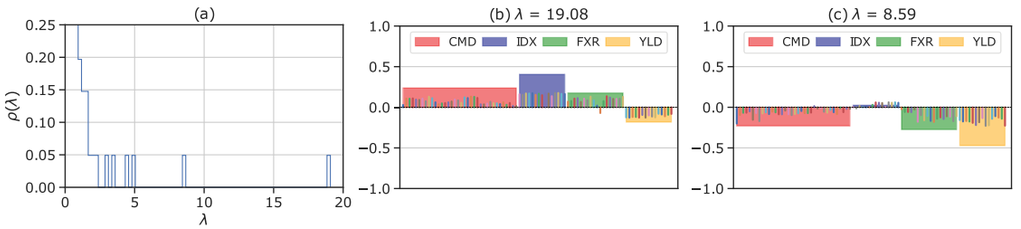

3 Principal regression analysis

3.1 A naive index factor

We first consider a linear statistical model similar to what is considered in Reigneron et al. (2011), only using the futures market sign-adjusted index I_0 defined in (3) instead of the mean index for stocks. We therefore consider a statistical model such that for each pair of futures indexed by i, j, the instantaneous correlation at time t is a linear function of the index τ days ago. More precisely, the hypothesized model reads:

$$\rho_{i,j}(t) = \mathbf{C}_{i,j} + \mathbf{D}_{i,j}(\tau) I_0(t-\tau) + \varepsilon_{i,j}(t,\tau)\,, \tag{8}$$

with $\rho_{i,j}(t) := r_i(t) r_j(t)$ and τ a certain lag that we will take to be equal to 1 day in the present section. The plot of Figure 3 makes the case for hypothesizing such a statistical model: it shows the value of the average signed correlations, defined as

$$\overline{\rho}(t) = \frac{1}{N(N-1)} \sum_{i \neq j} s_i s_j \rho_{i,j}(t) \tag{9}$$

as a function of the past-day index $I_0(t-1)$. A negative, close-to-linear relationship is clearly visible. Given that $N\overline{\rho}(t)$ can be written as $\mathbf{e}_0 \cdot \boldsymbol{\rho}(t)\mathbf{e}_0 \approx \mathbf{v}_1^{\boldsymbol{\rho}}(t) \cdot \boldsymbol{\rho}(t)\mathbf{v}_1^{\boldsymbol{\rho}}(t) = \lambda_1^{\boldsymbol{\rho}}(t)$, this motivates the fact that (8) is a reasonable model, as there is a simple linear relationship between $\lambda_1^{\boldsymbol{\rho}(t)}$ and $\lambda_N^{\mathbf{D}}$ – see (10) below.

For a given τ, the slope coefficients $\mathbf{D}_{i,j}(\tau)$ are determined by ordinary least squares (OLS). As alluded to in the Introduction, $\langle I \rangle = 0$ ensures that the intercept is precisely the i,j entry of the empirical correlation matrix $\mathbf{C}$.

Figure 3: Average (signed) correlation $\overline{\rho}(t)$, defined in (9), as a function of the past-day index $I_0(t-1)$. The plot is obtained by binning and averaging values of $\overline{\rho}(t)$ over five ranges of $I_0(t-1)$ of equal length, $(\max I_0(t-1) - \min I_0(t-1))/5$.

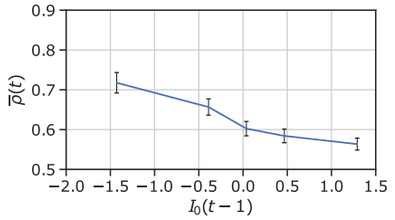

The plots in Figure 4 depict the obtained $\mathbf{D}(\tau = 1)$ matrix (simply denoted by $\mathbf{D}$ in the following), which exhibits a remarkable structure. Its ranked-eigenvalue spectrum is depicted in Figure 5(a), superposed on the null-hypothesis spectrum.[2] We find in particular that the most negative eigenvalue $\lambda_N^{\mathbf{D}}$ is highly significant, and equal to -3.1 ($p = 0.01$). All other eigenvalues are not significant.

As far as eigenvectors are concerned, $\mathbf{v}_N^{\mathbf{D}}$ is represented in Figure 5(c). We find that $\mathbf{v}_1^{\mathbf{C}} \cdot \mathbf{v}_N^{\mathbf{D}} = 0.93$ ($p = 0.01$), this quantity being represented along with the cumulative distribution function (CDF) of the corresponding null quantity in Figure 5(d). Hence, $\mathbf{v}_N^{\mathbf{D}}$ is nearly co-linear with the top eigenvector of $\mathbf{C}$. We also find that all other pairs $|\mathbf{v}_i^{\mathbf{C}} \cdot \mathbf{v}_j^{\mathbf{D}}|$ are much smaller than unity and not significant.

Figure 4: (a) $\mathbf{D}$ matrix obtained by fitting the statistical model (8). (b) Subsector-averaged version. (c) Sector-averaged version.

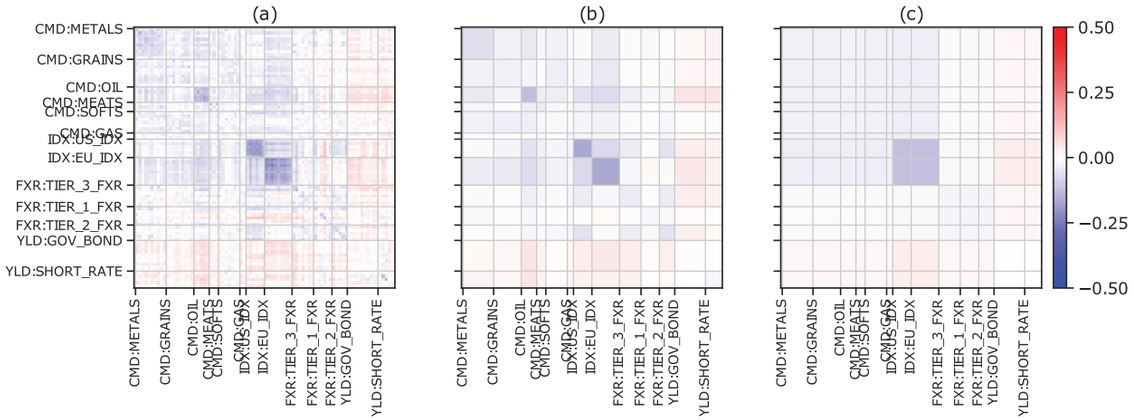

Figure 5: (a) Spectrum of the $\mathbf{D}(\tau = 1)$ matrix obtained by fitting the statistical model (8), superposed on the spectrum of the null hypothesis. (b) λ_N^D and its corresponding CDF in the null-hypothesis case. (c) Visual representation of $\mathbf{v}_N^D$. (d) Its overlap with the market mode $\mathbf{v}_1^C$ and the CDF of the corresponding quantity in the null-hypothesis case.

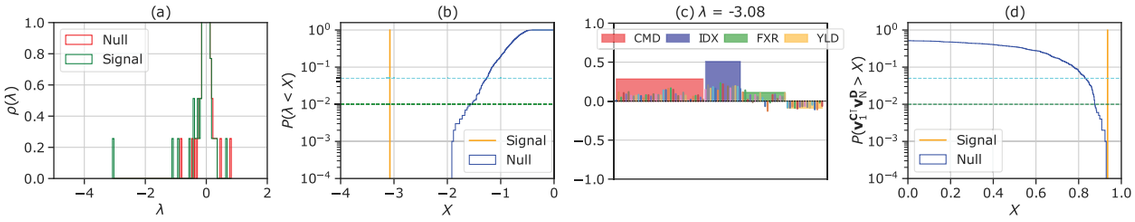

Hence, we find that the instantaneous correlation matrix $\rho_{ij}(t)$ has all its eigenvectors and eigenvalues essentially independent of $I_0(t-1)$, *except for the top eigenvalue*, which can be written as

$$\lambda_1^{\rho}(t) \approx \lambda_1^{\mathbf{C}} + I_0(t-1)\lambda_N^{\mathbf{D}}(\mathbf{v}_1^{\mathbf{C}} \cdot \mathbf{v}_N^{\mathbf{D}})^2. \tag{10}$$

In other words, a negative (resp. positive) past index tends to increase (resp. decrease) the largest eigenvalue of the correlation matrix, i.e. increase (resp. decrease) local correlations between futures that are correlated in the market mode and increase (resp. decrease) anti-correlations between anti-correlated ones. Since $\mathbf{v}_1^{\mathbf{C}} \cdot \mathbf{v}_N^{\mathbf{D}} \approx 1$, the behavior of I_0 hardly changes the direction of the top eigenvector. If anything, the top eigenvector $\mathbf{v}_1^{\boldsymbol{\rho}(\mathbf{t})}$ of the corrected correlation matrix $\rho(t)$ deviates from the uniform mode for negative past-day values of I_0, an effect even more pronounced for positive values of this index. These results can be inferred from the plot in Figure 6. This behavior of the futures market is in contrast to that of stocks presented in Reigneron et al. (2011), for which negative index values resulted in the market mode rotating towards the uniform mode in the subsequent days.

We also find that eigenvectors of $\mathbf{D}$ other than $\mathbf{v}_1^{\mathbf{D}}$ do not lie in a subspace spanned by a simple subset of $\mathbf{C}$'s eigenvectors, neither are they easily interpretable in terms of sectors. For example, to generate a vector such that its dot product with $\mathbf{D}$'s second eigenvector is greater than 0.9, we need to include at least five higher-order eigenvectors of $\mathbf{C}$.

Yet, the matrix plots of Figure 4 give some insight about the distribution of the correlations correction across different futures. In particular, it is clear that

Figure 6: Angle between the instantaneous, I_0-dependent correlation matrix top eigenvector and the uniform mode $\mathbf{e_0}$ compared to the angle between the unconditional correlation matrix top eigenvector $\mathbf{v}_1^{\mathbf{C}}$ with $\mathbf{e_0}$. The $\angle$ symbol denotes the $\arccos$ function. We measure $\angle(\mathbf{e_0}, \mathbf{v}_1^{\mathbf{C}}) = 0.45$ rad.

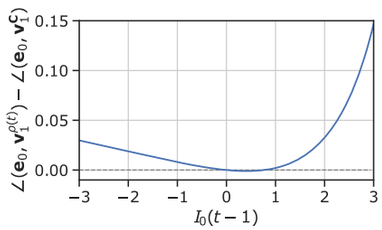

correlations between assets from the IDX sector tend to increase more than others for a given level of negative past-day index.

3.2 Exponential moving average index

We now consider a modified index that is weighted by an exponentially decreasing kernel. More precisely, we define

$$J_\beta(t) := \sum_{s=0}^{T_k} I_0(t-s)\mathrm{e}^{-\beta s} \tag{11}$$

Figure 7: Evolution of some of $\mathbf{D}_\beta$'s spectral characteristics as a function of the decay time β^{-1}. (a) $\mathbf{D}_\beta$'s most negative eigenvalue. (b) Dot product of associated eigenvector with the market mode $\mathbf{v}_1^{\mathbf{C}}$. (c) $\mathbf{D}_\beta$'s most positive eigenvalue; (d) Dot product of associated eigenvector with the market mode $\mathbf{v}_1^{\mathbf{C}}$. All gray zones indicate non-significant values down to $p = 0.05$ level. Orange dashed lines represent the value of the corresponding quantity for $\mathbf{D}(\tau = 1)$.

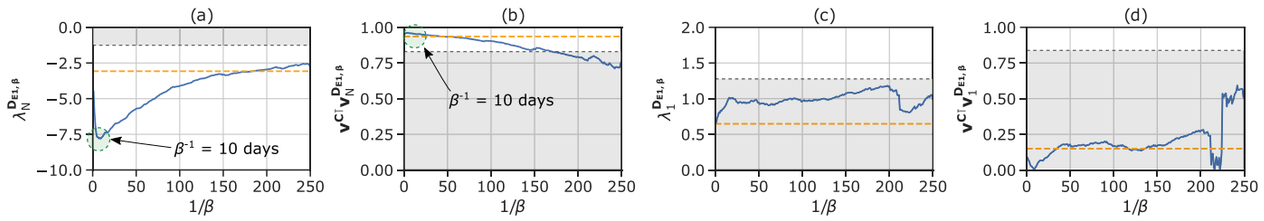

Figure 8: (a) $\mathbf{D}_\beta$ matrix obtained by fitting the statistical model (8), with J_β in place of I_0 and for the optimal timescale parameter $\beta^{-1} = 10$ days. (b) Subsector-averaged version. (c) Sector-averaged version.

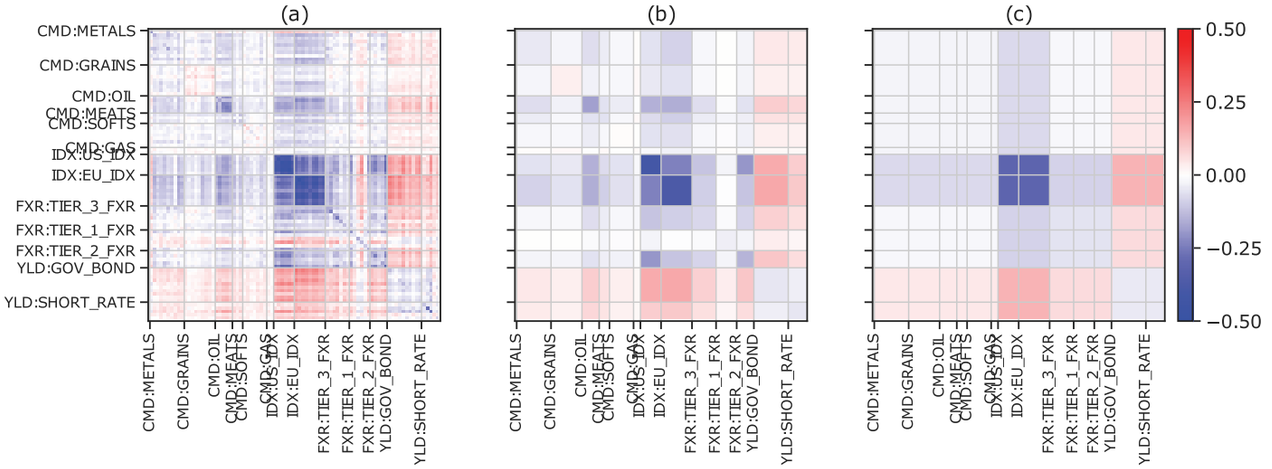

Figure 9: (a) Spectrum of the $\mathbf{D}_\beta$ matrix obtained by fitting the statistical model (8), with J_β in place of I_0, where $\beta = 0.1$, the optimal timescale. This spectrum is superposed on that of the null-hypothesis case. (b) $\lambda_{\mathrm{N}}^{\mathbf{D}_\beta}$ and its corresponding CDF in the null-hypothesis case. (c) Visual representation of $\mathbf{v}_{\mathrm{N}}^{\mathbf{D}_\beta}$. (d) Its overlap with the market mode $\mathbf{v}_1^{\mathbf{C}}$ and the CDF of the corresponding quantity in the null-hypothesis case.

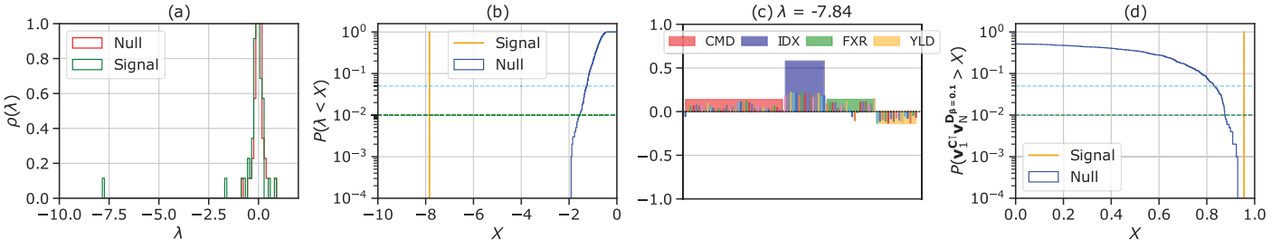

where T_{k} is the cutoff time defined as $T_{\mathrm{k}} = \beta^{-1}\log(100)$, such that $e^{-\beta T_k} = 0.01$. Again, we further normalize $J_\beta(t)$ so that it has unit variance. The corresponding $\mathbf{D}_\beta$ is then obtained by fitting model (8) with $I_0(t-1)$ replaced by $J_\beta(t-1)$.

Figure 7(a) shows the evolution of $\mathbf{D}_\beta$'s most negative eigenvalue against the value of the decay time β^{-1}, while the alignment of the associated eigenvector with the market mode $\mathbf{v}_1^{\mathbf{C}}$ is depicted in Figure 7(b). From these plots, we can infer that a timescale of $\beta^{-1} = 10$ days maximizes the magnitude of the effect. The largest *positive* eigenvalue of $\mathbf{D}_\beta$, in contrast, doesn't reveal any notable features, see Figures 7(c) and (d). In the following, $\mathbf{D}_\beta$ denotes $\mathbf{D}_{\beta=0.1}$.

The matrix $\mathbf{D}_{\beta=0.1}$ is depicted in Figure 8, and some important spectrum characteristics are shown in Figure 9. Both the value of the most negative eigenvalue and of the dot product with the market mode are increased compared to the instantaneous case $\mathbf{D}(\tau = 1)$: we measure $\lambda_{\mathrm{N}}^{\mathbf{D}_\beta} = -7.8$ $(p < 0.01)$ and $\mathbf{v}_1^{\mathbf{C}} \cdot \mathbf{v}_{\mathrm{N}}^{\mathbf{D}_\beta} = 0.96$ $(p < 0.01)$. As expected, the feedback between past market

Figure 10: Evolution of some of $\mathbf{D}_{E_\beta}$'s spectral characteristics as a function of the timescale parameter β^{-1}. (a) $\mathbf{D}_{E_\beta}$'s smallest eigenvalue. (b) Dot product of associated eigenvector with the market mode $\mathbf{v}_1^{\mathrm{C}}$. (c) $\mathbf{D}_{E_\beta}$'s largest eigenvalue. (d) Dot product of associated eigenvectors with the market mode $\mathbf{v}_1^{\mathrm{C}}$. All grayed zones indicate non-significant values to the $p = 0.05$ level. Orange dashed lines represent the value of the associated quantity for $\mathbf{D}_E$, the matrix obtained by fitting the statistical model (13) with the instantaneous index (obtained by taking $T_k = 0$ in (12)).

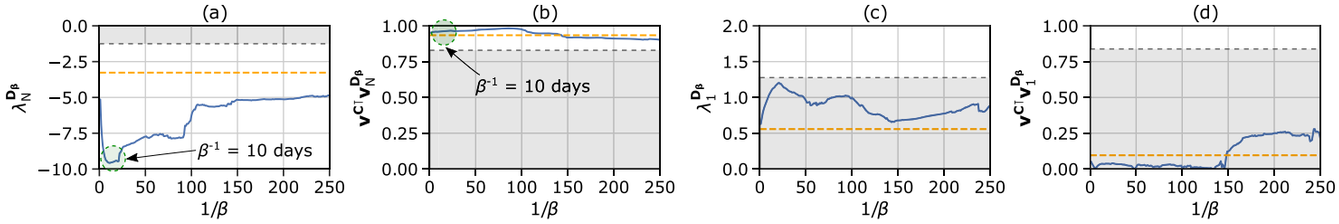

Figure 11: (a) $\mathbf{D}_{E_\beta}$ matrix obtained by fitting the statistical model (13) with optimal timescale parameter $\beta^{-1} = 10$ days. (b) Subsector-averaged version. (c) Sector-averaged version.

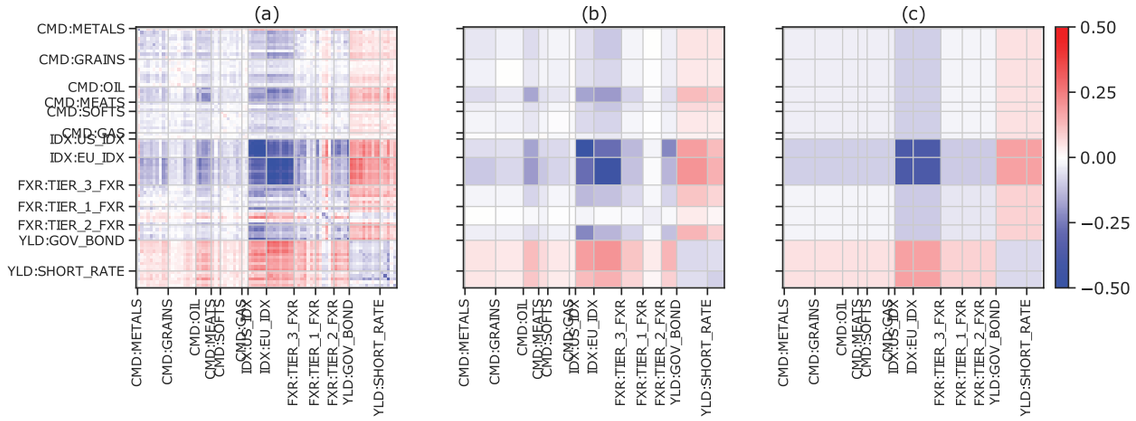

behavior and future correlations takes some time to build up; we find that 10 trading days (2 weeks) is the order of magnitude of this reaction time.

Note that all other eigenvalues (in particular positive eigenvalues) and dot products are much smaller in absolute value, and therefore not significant, as in Section 3.1.

3.3 The "eigenfactor"

Elaborating on the previous results, we now construct our final indicator, which relies on the local correlation matrix $\mathbf{C}_K(t)$, based on the recent past returns between $t - K$ and $t - 1$.

We chose $K = 3N$ (days) as a trade-off between finite-size noise and non-stationarity effects. For each t, the top eigenvector $\mathbf{v}_1^{\mathbf{C}_K}(t)$ of $\mathbf{C}_K(t)$ is determined. The exponentially smoothed "eigenfactor" is then computed as

$$E_\beta(t) = \sum_{s=0}^{T_k} \mathbf{r}(t) \cdot \mathbf{v}_1^{\mathbf{C}_K}(t)\, \mathrm{e}^{-\beta s}. \tag{12}$$

We again make sure that E_β is centered and standardized.

We consider the eigenfactor $E_\beta(t)$ as a more precise version of $J_\beta(t)$, obtained by fine-tuning each future contract in the index according to its weight in the local market mode while enforcing causality (instead of the ± 1 weights in $I_0(t)$). This procedure does not require ad-hoc changes of sign, like we did for the YLD sector (which might actually change again in the future, as it changed in 1997). Another "anomaly" that can be detected in Figure 1 is the YEN vs. USD, with a correlation with the IDX sector at odds with other currencies. All these idiosyncracies are automatically accounted for with the eigenfactor $E_\beta(t)$.

The statistical model for the PRA associated with this eigenfactor reads

$$\boldsymbol{\rho}(t) = \mathbf{C} + \mathbf{D}_{E_\beta} E_\beta(t-1) + \boldsymbol{\varepsilon}\,. \tag{13}$$

We first carry out a sensitivity analysis of the dominant eigenvalues of the obtained $\mathbf{D}_{E_\beta}$ matrices against the β parameters. The results are depicted in Figure 10, and advocate for a choice of the optimal timescale parameter $\beta = 0.1$, which coincides with that of the J_β factor. In the following, $\mathbf{D}_E$ will denote $\mathbf{D}_{E_{\beta=0.1}}$.

Let us now describe the results of the PRA using the eigenfactor $E_\beta(t)$ with this optimal timescale parameter. The matrix $\mathbf{D}_E$ obtained by fitting the statistical model (13) with the optimal timescale parameter $\beta = 0.1$ is depicted in Figure 11. Note that the structure of $\mathbf{D}_E$ appears much more markedly than within our previous two attempts, cf. Figures 4 and 8. The spectral characteristics of $\mathbf{D}_E$ are shown in Figure 12. These results indicate that the $E_\beta(t)$ index leads to a significantly stronger effect than what we observed with $J_\beta(t)$. In particular, we measure $\lambda_{\mathrm{N}}^{\mathbf{D}_{\mathrm{E}}} = -9.56$ ($p < 0.01$) and $\mathbf{v}_1^{\mathbf{C}} \cdot \mathbf{v}_{\mathrm{N}}^{\mathbf{D}_{\mathrm{E}}} = 0.96$ ($p < 0.01$), to be compared with, respectively, -7.8 and 0.96

Figure 12: (a) Spectrum of the $\mathbf{D}_E$ matrix obtained by fitting the statistical model (13), where $\beta = 0.1$, the optimal timescale. This spectrum is superposed on that of the null-hypothesis case. (b) Value of $\lambda_{\mathrm{N}}^{\mathbf{D}_{\mathrm{E}}}$ and its corresponding CDF in the null-hypothesis case. (c) Visual representation of $\mathbf{v}_{\mathrm{N}}^{\mathbf{D}_{\mathrm{E}}}$. (d) Its overlap with the market mode $\mathbf{v}_1^{\mathbf{C}}$ and the CDF of the corresponding quantity in the null-hypothesis case.

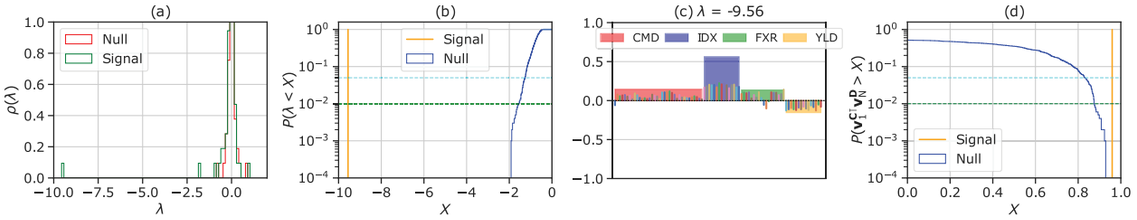

Figure 13: Angle between the instantaneous, E_β-dependent correlation matrix top eigenvector and the uniform mode $\mathbf{e}_0$ compared to the angle between the unconditional correlation matrix top eigenvector $\mathbf{v}_1^{\mathbf{C}}$ with $\mathbf{e}_0$. The $\angle$ symbol denotes the arccos function. We measure $\angle(\mathbf{e}_0, \mathbf{v}_1^{\mathbf{C}}) = 0.45$ rad. Note that for moderately positive eigenfactor $E_\beta(t-1) \in [0;1]$, the top eigenvector rotates *towards* $\mathbf{e}_0$.

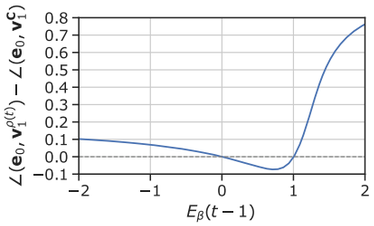

for J_β. All other eigenvalues (in particular positive eigenvalues) and dot products are again significantly smaller in absolute value and can be neglected.

As for the index I_0, we measure the difference in deviation of $\rho_{ij}(t)$'s top eigenvector from the uniform mode $\mathbf{e}_0$. The results are depicted in Figure 13. The results are qualitatively the same as for the I_0 index: when the eigenfactor moves, the top eigenvector of $\rho_{ij}(t)$ moves *away* from the uniform mode $\mathbf{e}_0$, except for a small region of $E_\beta(t-1) \in [0;1]$ where it rotates towards $\mathbf{e}_0$.

4 Zooming-in: sector indicators

In order to break down the effect reported above into different sector contributions, we now carry out a PRA using corresponding sub-indexes as indicators. More precisely, we consider the mean return of each sector over timescale β^{-1}, and hypothesize the following statistical model:

$$\boldsymbol{\rho}(t) = \mathbf{C} + \sum_{F \in \mathcal{F}} \mathbf{D}_{\mathrm{F}} I_{\mathrm{F},\beta}(t-1) + \boldsymbol{\varepsilon}\,, \tag{14}$$

with the notation defined in Section 2. Again, we chose the value $\beta^{-1} = 10$ days for the time-decay parameter in the following analysis (chosen equal for all sectors).

The spectra of the $\mathbf{D}_{\mathrm{F}}$ matrices are represented in Figure 14. The dot products of the eigenvectors corresponding to the extreme eigenvalues with the market mode $\mathbf{v}_1^{\mathbf{C}}$ are also reported in the figure. The results show that the only eigenvalues and eigenvectors that carry both value and direction significance are the IDX smallest eigenvalue $\lambda_{\mathrm{N}}^{\mathbf{D}_{\mathrm{IDX}}} = -8.5$ ($p < 0.01$) and the YLD largest eigenvalue $\lambda_1^{\mathbf{D}_{\mathrm{YLD}}} = 3.9$ ($p < 0.01$). The impact on the correlations following the market mode is then clear through

$$\lambda_1^{\boldsymbol{\rho}}(t) \approx \lambda_1^{\mathbf{C}} + I_{\mathrm{IDX},\beta}(t-1)\lambda_{\mathrm{N}}^{\mathbf{D}_{\mathrm{IDX}}}(\mathbf{v}_1^{\mathbf{C}} \cdot \mathbf{v}_{\mathrm{N}}^{\mathbf{D}_{\mathrm{IDX}}})^2 + I_{\mathrm{YLD},\beta}(t-1)\lambda_1^{\mathbf{D}_{\mathrm{YLD}}}(\mathbf{v}_1^{\mathbf{C}} \cdot \mathbf{v}_1^{\mathbf{D}_{\mathrm{YLD}}})^2, \tag{15}$$

which shows that negative (resp. positive) past IDX index increases (resp. decreases) the correlations along the market mode, while the opposite holds for the past YLD index. However, the magnitude of the effect is approximately two times larger for the IDX index compared to the YLD index, given the relative values of $\lambda_{\mathrm{N}}^{\mathbf{D}_{\mathrm{IDX}}}$ and $\lambda_1^{\mathbf{D}_{\mathrm{YLD}}}$.

Given the low magnitude of their eigenvalues, and the unclear direction of their eigenvectors, the effect of the CMD and FXR sector indexes is more difficult to interpret: their overlap with the market mode $\mathbf{v}_1^{\mathbf{C}}$ is small. Therefore, quantifying the effect of these indexes on the correlations $\rho(t)$ in an interpretable manner requires identifying a low-dimensional subspace in which the top eigenvectors of $\mathbf{D}_{\mathrm{FXR}}$ or $\mathbf{D}_{\mathrm{CMD}}$ live, in the basis of $\mathbf{C}$'s eigenvectors. But as was the case in Section 3.1 for higher modes of the $\mathbf{D}$ matrix, we find that the subspaces in which the corresponding eigenvectors live have no simple interpretations.

5 Summary and conclusion

This paper shows that the correlation matrix describing the co-evolution of futures contracts depends significantly on the past return of the "futures market mode" (where stock indexes, commodities, and currencies have a +1 weight and bonds a −1 weight). More precisely, our results suggest that negative past returns of this futures market mode lead to an increased forward average correlation. This effect is even more prominent if one considers the so-called "eigen-factor", an average index that finely weights each future contract according to its weight in the empirical correlation matrix dominant eigenmode. We have also identified that an exponential moving average of both indexes with a characteristic timescale of about 10 days maximizes its explanatory power for changes in future average correlations.

Sectorial indexes give us a finer picture of the futures market's index leverage effect, as our analysis indicates that the mean variations of returns within different sectors have different effects on the future correlations, both in sign and magnitude. Namely, past market movements within the indexes (IDX) sector are negatively correlated with a given day's instantaneous correlations, while the opposite is true for the bonds (YLD) sector. As the indexes and bond sectors are anti-correlated in the market mode, the sectorial indexes give us a consistent decomposition of the results that were obtained with simple indexes. Moreover, this decomposition gives us a quantitatively finer picture of each sector's contribution to the average correlation movements, with the indexes sector having twice the effect on the correlations on average as the bonds sector.

Figure 14: Spectra of the $\mathbf{D_F}$ matrices obtained by fitting the statistical model (14). The numbers reported on top of the extreme eigenvalues give the value of the dot product between the corresponding eigenvector and the market mode $\mathbf{v_1^C}$.

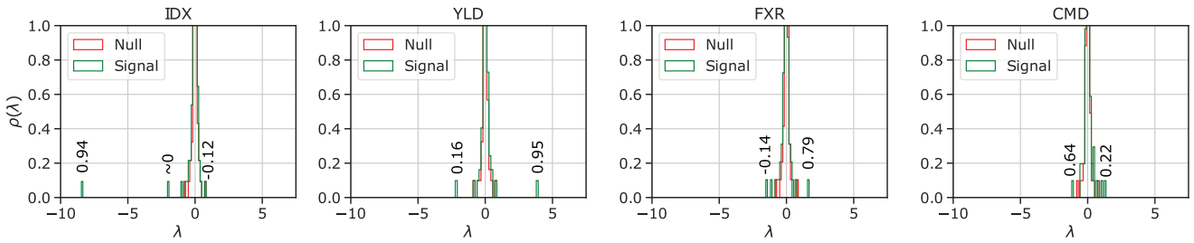

This paper calls for subsequent investigations in several directions. Firstly, the predictive power of the linear PRA could be tested using e.g. an out-of-sample score of the risk as obtained with a PRA-fitted linear model, such as (8) or (14). This score can then be compared to that obtained through an uncorrected empirical matrix, to assess whether one would gain by using the PRA models for risk estimation purposes in non-stationary regimes. Secondly, the identification of the various predictors considered in this paper opens the path to using them as features in more complex correlations and risk assessment models (e.g. neural networks). Finally, it would be interesting to decompose the effect exposed in this paper into a local volatility contribution (which our local volatility normalization does not remove entirely) and a genuine local correlation contribution. Work in this direction is underway (Morel et al., 2020).

Appendix

List of futures

In this appendix, we provide the list of futures used in this study. We organize these contracts by sector, and by market on which they are traded. This list is reported in Table A1.

Table A1: List of futures ordered by sectors and markets

Sector	IDX (indexes)	YLD (bonds)	FXR (currencies)	CMD (commodities)
Market				
Chicago Mercantile Exchange	E-mini Russell 2000 Index Futures, E-Mini NASDAQ 100 Index Future, E-Mini S&P's MidCap 400 Index Future, E-Mini S&P's 500 Index Future	3 Month Eurodollar Future	Australian Dollar Currency Future, Brazilian Real Currency Future, Canadian Dollar Currency Future, Swiss Franc Currency Future, Euro Foreign Exchange Currency Future, British Pound Currency Future, Japanese Yen Currency Future, Mexican Peso Currency Future, New Zealand Dollar Currency Future, South African Rand Currency Future	Feeder Cattle Future, Live Cattle Future, Lean Hogs Future

Table A1: Contnued

Sector	IDX (indexes)	YLD (bonds)	FXR (currencies)	CMD (commodities)
Market				
Chicago Board of Trade	Mini Dow Jones Industrial Average e-CBOT Future	10 Year US Treasury Note Future, 2 Year US Treasury Note Future, 5 Year US Treasury Note Future, US Long Bond Future		Corn Future, Hard Red Winter Wheat Future, Soybean Meal Future, Soybean Oil Future, Soybean Future, Wheat Future
New York Mercantile Exchange				Light Sweet Crude Oil Future, NY Harbor ULSD Futures, Henry Hub Natural Gas Futures, Palladium Future, Platinum Future, Reformulated Gasoline Blendstock for Oxygen Blending RBOB Futures
Commodity Exchange, Inc.				Copper Future, Gold 100 Troy Ounces Future, Silver Future
Eurex	DAX Index Future, EURO STOXX 50 Future, Swiss Market New Index Future	5 Year Euro BOBL Future, 10 Year Euro BUND Future, 30 Year Euro BUXL Future, 2 Year Euro SCHATZ Future		
Euronext Derivatives Paris	Amsterdam Index Future, CAC 40 Index Future			Rapeseed Future, Milling Wheat Future
ICE Futures	FTSE 100 Index Future	3 Month Euro Euribor Future, 3 Month Euroswiss Future, Long Gilt Future, 90 Day Sterling Future		Brent Crude Oil Future, Canola Future, Cocoa Future, Gas Oil Future, Robusta Coffee Future 10-Tonne, White Sugar Future, Natural Gas Future, C Coffee Future, Number 2 Cotton Future, Number 11 World Sugar Future, Frozen Concentrated Orange Juice A Future

Table A1: Contnued

Sector	IDX (indexes)	YLD (bonds)	FXR (currencies)	CMD (commodities)
Market				
London Metal Exchange				Aluminum, Lead, Nickel, Tin, Zinc
Montreal Exchange	S&P/TSX 60 Index Future	10 Year Canadian Bond Future, 3 Month Canadian Bank Acceptance Future		
Meff Renta Variable (Madrid)	Madrid IBEX 35 Index Future			
Borsa Italiana (IDEM)	FTSE/MIB Index Future			
South African Futures Exchange	FTSE/JSE Top 40 Index Future			
Forward market			Czech Koruna, Hungarian Forint, Israeli New Shekel, Norwegian Krone, Poland Zloty, Swedish Krona, Singapore Dollar, Turkish Lira	

Acknowledgments

This research was conducted within the Econophysics & Complex Systems Research Chair, under the aegis of the Fondation du Risque, the Fondation de l'Ecole polytechnique, the Ecole polytechnique, and Capital Fund Management. We thank Rudy Morel for very useful discussions.

Armine Karami received MSc and PhD degrees in electrical engineering from Sorbonne Université in 2014 and 2018. His PhD was focused on the theory and analysis of electrostatic kinetic energy harvesting systems. He is now part of the Econophysics and Complex Systems team at LadHyX, Ecole polytechnique, Palaiseau, France, as a postdoctoral researcher. There, he conducts research in quantitative finance and economics on the cleaning of large covariance matrices using statistical learning.

Raphaël Benicho obtained his PhD in theoretical physics from Université Pierre et Marie Curie in 2009. He joined the Superstring Theory research group at Vrije Universiteit Brussel between 2009 and 2012 as a post-doctoral researcher. He is working as a researcher at Capital Fund Management since 2012.

Michael Benzaquen obtained his PhD in theoretical physics from Université Pierre et Marie Curie in 2015. His curiosity took him to Capital Fund Management (CFM) where he worked alongside Jean-Philippe Bouchaud on market microstructure related issues. He was then appointed by the CNRS at Ecole Polytechnique in 2016 as a tenured researcher, and associate professor in the department of economics. His research interests include quantitative finance, economics and complex systems in general, from a physical perspective. He is a visiting scholar at Capital Fund Management (CFM) where he collaborates with the execution team on execution related issues. In 2017 he co-founded Art in Research, the first art gallery devoted to scientific photography. In 2018, he founded, and currently heads, the CFM Chair of Econophysics and Complex Systems at Ecole Polytechnique. Besides, he teaches financial markets and statistical physics of social sciences at ENSAE ParisTech and Ecole Polytechnique.

Jean-Philippe Bouchaud studied at the French Lycée of London, and graduated from the Ecole Normale Supérieure in Paris, where he also obtained his PhD in physics. He was then appointed by the CNRS until 1992. After a year spent in the Cavendish Laboratory (Cambridge), he joined the Service de Physique de l'Etat Condensé (CEA-Saclay), where he worked on the dynamics of glassy systems and on granular media. He became interested in economics and theoretical finance in 1991. His work in finance includes extreme risk models, agent-based simulations, market microstructure and price formation. He has been very critical about the standard concepts and models used in economics and in the financial industry (market efficiency, Black-Scholes models, etc.). He founded the company Science & Finance in 1994 that merged with Capital Fund Management (CFM) in 2000. He is the President and Head of Research at CFM and professor at Ecole Polytechnique since 2008. He was awarded the IBM young scientist prize in 1990 and the C.N.R.S. Silver Medal in 1996. He has published over 250 scientific papers and several books in physics and in finance.

Endnote

1. This allows us to remove part of, but not all, local volatility fluctuations. The normalized returns are furthermore clipped between −5 and 5, to remove very extreme price changes and/or errors.
2. Throughout this paper, the null hypothesis is computed by averaging over 1000 $\mathbf{D}$-matrices, each of which is obtained by fitting the model (8) to a centered and standardized random predictor, independent of the returns, in place of $l_0(t-1)$ or $E_\beta(t-1)$.

References

[1] Ang, A. and Chen, J. 2002. Asymmetric correlations of equity portfolios. *Journal of Financial Economics* 63(3), 443–494.

[2] Balogh, E., Simonsen, I., Nagy, B. Z. and Néda, Z. 2010. Persistent collective trend in stock markets. *Physical Review E* 82(6), 066,113.
[3] Baur, D. G. and Lucey, B. M. 2009. Flights and contagion-an empirical analysis of stock–bond correlations. *Journal of Financial Stability* 5(4), 339–352.
[4] Bekaert, G. and Wu, G. 2000. Asymmetric volatility and risk in equity markets. *The Review of Financial Studies* 13(1), 1–42.
[5] Borland, L. 2012. Statistical signatures in times of panic: Markets as a self-organizing system. *Quantitative Finance* 12(9), 1367–1379.
[6] Bouchaud, J.-P., Matacz, A. and Potters, M. 2001. Leverage effect in financial markets: The retarded volatility model. *Physical Review Letters* 87, 228701.
[7] Bun, J., Bouchaud, J.-P. and Potters, M. 2017. Cleaning large correlation matrices: Tools from random matrix theory. *Physics Reports* 666, 1–109.
[8] Cont, R. 2001. Empirical properties of asset returns: Stylized facts and statistical issues. *Quantitative Finance* 1(2), 223–236.
[9] Engle, R. 2002. Dynamic conditional correlation: A simple class of multivariate generalized autoregressive conditional heteroskedasticity models. *Journal of Business & Economic Statistics* 20(3), 339–350.
[10] Li, Q., Yang, J., Hsiao, C. and Chang, Y.-J. 2005. The relationship between stock returns and volatility in international stock markets. *Journal of Empirical Finance* 12(5), 650–665.
[11] Morel, R., Bouchaud, J.-P. and Mallat, S. 2020. *Maximum-Entropy Scattering Models for Multivariate Financial Time Series (Technical Report)*, in preparation.
[12] Reigneron, P.-A., Allez, R. and Bouchaud, J.-P. 2011. Principal regression analysis and the index leverage effect, *Physica A: Statistical Mechanics and its Applications* 390(17), 3026–3035.
[13] Wyart, M., and Bouchaud, J.-P. 2007. Self-referential behaviour, overreaction and conventions in financial markets, *Journal of Economic Behavior & Organization* 63(1), 1–24.